Solar Energy Materials & Solar Cells 251 (2023) 112121

Contents lists available at ScienceDirect

Solar Energy Materials and Solar Cells

journal homepage: www.elsevier.com/locate/solmat

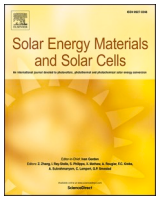

Investigation of light-induced degradation in gallium- and indium-doped Czochralski silicon

Saman Jafari *, Mieka Figg, Ziv Hameiri

The University of New South Wales, Sydney, NSW, 2052, Australia

ARTICLE INFO

Keywords:
Ga-doped Cz silicon
In-doped Cz silicon
Light-induced degradation
Lifetime degradation

ABSTRACT

Light-induced degradation (LID) in boron (B)-doped Czochralski (Cz) silicon wafers has impacted commercial *p*-type silicon solar cells for decades. Substitution of boron with gallium (Ga) or (to a lesser extent) indium (In) has been suggested as a method to tackle this problem since Ga- and In-doped Cz wafers were shown to be less prone to LID. Although less prone to LID, several studies have reported some LID in these materials. In this study, LID in Ga- and In-doped Cz wafers is investigated. First, it is shown that LID is present in both materials. The degradation has two stages (fast and slow) for Ga-doped wafers and one stage for In-doped wafers. By performing the degradation at different temperatures, the activation energy of the defect formation is determined to be 0.74 ± 0.10 eV for the slow step in Ga-doped and 0.91 ± 0.15 eV for In-doped wafers. We then investigate defect deactivation with dark annealing. Both Ga- and In-doped wafers demonstrate a two-stage defect deactivation. Similar to defect formation, the defect deactivation activation energies are determined and reported. Finally, the focus is shifted to investigating the degradation mechanism in Ga-doped wafers, since they are currently the dominating wafer substrate for photovoltaic applications. It is shown that a three-state mechanism ("annealed", "degraded", and "stabilised"), similar to boron-oxygen (BO)-related defects, can explain their degradation. It seems the four-state model, suggested for the light- and elevated temperature-induced degradation, is not suitable for describing the degradation in Ga-doped Cz wafers.

1. Introduction

Light-induced degradation (LID) in boron (B)-doped Czochralski (Cz)-grown wafers has affected cells made from this material for decades [1]. A possible solution to prevent the negative impact of LID on cell efficiencies is to substitute boron with other dopants from Group III, such as aluminium (Al), gallium (Ga), or indium (In). The strong recombination activity of Al-oxygen (O) pairs in Cz silicon makes Al a less viable option [2]. Both Ga and In have been investigated as dopants to produce industrial *p*-type silicon [3,4]. Ga has a segregation coefficient of 8×10^{-3} and ionisation energy of 0.065 eV, while the values for In are 4×10^{-4} and 0.156 eV, respectively [5,6]. Since a higher segregation coefficient leads to a better uniformity of doping throughout the ingot and as lower ionisation energy results in a lower resistivity at the operating temperatures, Ga is preferred over In. Consequently, the industry has shifted towards Ga-doped wafers and currently more than 90% of the *p*-type Cz wafers used for photovoltaic (PV) applications are Ga-doped wafers [7].

The conclusions of studies regarding the presence of LID in Ga-doped wafers are yet not conclusive [4,8–10]. Some investigations have suggested negligible or no LID in Ga-doped wafers [4,8,11]. However, other studies reported degradation after light soaking [9,10,12]. Nevertheless, it is suggested that the extent of LID in Ga-doped wafers is smaller than in B-doped wafers and occurs over longer time scales [9]. Note that most of the studies that investigated degradation in Ga-doped wafers have used the term light- and elevated temperature-induced degradation (LeTID) to describe this phenomenon. However, in this study, we use the more general term LID and the reason for this choice will be discussed in the next section. It was shown that similar to both LID and LeTID, a prolonged light soaking results first in the degradation and then in the recovery of the lifetime while further light soaking does not further degrade the lifetime [9,13,14]. The firing step appears to be crucial to observing LID in Ga-doped wafers [15,16]. Also, the thermal history of the wafers or cells seems to have a significant impact on the LID behaviour. Grant et al. found that dark annealing of Ga-doped solar cells in the temperature range between 200 °C and 300 °C *before* the light soaking, increases the LID extent [9]. It has been also shown that LID behaviour depends on the injection level during illumination [17].

* Corresponding author.
E-mail address: edu.saman.jafari@gmail.com (S. Jafari).

https://doi.org/10.1016/j.solmat.2022.112121
Received 31 August 2022; Received in revised form 1 November 2022; Accepted 17 November 2022
Available online 29 November 2022

While for Ga-doped Cz wafers (1.0 Ω cm resistivity) a minor degradation was observed under 1-sun illumination at 75 °C, the samples were significantly degraded at the same temperature when illuminated at 0.1-sun [17]. This is different from LID in B-doped wafers where the degradation is independent of the light intensity for intensities higher than 0.01 suns [13]. It was shown that similar to the LID of B-doped silicon, dark annealing results in the lifetime recovery, causing the defects to return to their precursor form [12]. The impact of prolonged dark annealing on the lifetime of Ga-doped wafers has been investigated as well [17]. Dark annealing at 175 °C results in degradation after ~100 h, however, it was suggested that the defect causing this degradation is not the same as the LID-related defect [17].

The conclusions regarding the presence of LID in In-doped Cz silicon are also divided. While LID in In-doped wafers has been reported in some studies [18,19], no degradation has been observed in another investigation [20].

While several studies have investigated LID in Ga- and In-doped wafers, the mechanism responsible for the degradation in these materials is still unclear. To fill this knowledge gap, the change in the lifetime of two sets of Ga- and In-doped samples during light soaking is studied. Later, the defect formation rates are determined at different temperatures and the defect formation activation energies are extracted. Next, the defect deactivation with dark annealing is investigated and subsequently, the activation energies for defect deactivation are estimated. The focus is then shifted to only Ga-doped wafers. Using consecutive degradation, regeneration, and dark annealing cycles, a mechanism for LID in Ga-doped wafers is suggested.

2. Materials and methods

Two sets of Ga-doped wafers (Ga-1 and Ga-2) from different suppliers were used in this study with thicknesses of 189 ± 3 μm (Ga-1) and 164 ± 2 μm (Ga-2), and resistivities of 1.80 ± 0.04 Ω cm (Ga-1) and 0.78 ± 0.02 Ω cm (Ga-2). To investigate LID in the In-doped Cz wafers, a set of wafers with a thickness of 166 ± 3 μm and resistivity of 3.30 ± 0.12 Ω cm was used. All the wafers were gettered using a phosphorus diffusion at 840 °C for 45 min. The diffused layer was then etched off and the wafers were passivated using a plasma-enhanced chemical vapour deposition (PECVD) system. Ga-1 and In-doped sets were passivated with a 75-nm silicon nitride (SiN_x), with a refractive index of 2.08 at 632 nm [21] while the Ga-2 set was passivated with an aluminium oxide (AlO_x)-SiN_x stack. The extracted saturation current density (J_0) for the Ga-1 and In-doped sets is ~100 fA/cm^2 (at $\Delta n = 10^{16}$ cm^{-3} where Δn is the excess carrier concentration) while it is ~60 fA/cm^2 for the Ga-2 set (at $\Delta n = 2 \times 10^{16}$ cm^{-3}). After passivation, the wafers were fired at a peak set temperature of 900 °C using a SCHMID belt furnace. For the degradation process, the samples were illuminated at various temperatures using halogen lamps with 0.4 suns or 0.1 suns equivalent intensity. For dark annealing, the samples were annealed on a hot plate at various temperatures in the range of 140 °C–230 °C. The reported temperature during the halogen-based degradation and the dark annealing process is the sample temperature as measured by two k-type thermocouples (CHAL-005 OMEGA) attached to a sample from the same set that was located near the investigated sample. Besides halogen lamps, some of the samples were laser annealed at 140 °C (set temperature) using a 938 nm laser with 26 suns intensity for fast degradation and regeneration.

For the lifetime measurements, a Sinton Instrument WCT-120 lifetime tester was used. The normalised defect density (NDD) was calculated using:

$$NDD = \frac{1}{\tau_{deg(t)}} - \frac{1}{\tau_{DA}} \quad (1)$$

where $\tau_{deg(t)}$ is the effective lifetime after light soaking for t minutes and τ_{DA} is the effective lifetime after lifetime recovery with dark annealing. As mentioned before, after dark annealing the defects are not recombination-active, hence, the lifetime recovers as the defect density is very low. To fit the NDD curves during the defect formation, a single- or double-exponential function was used, and the defect formation rate (R_{deg}) was extracted:

$$NDD = N_{max}\left(1 - e^{-t\times R_{deg}}\right) \text{ or } NDD = a\left(1 - e^{-t\times R_{deg1}}\right) + b\left(1 - e^{-t\times R_{deg2}}\right) \quad (2)$$

where N_{max} is the maximum defect density, and a and b are the pre-exponential factors and $a + b = N_{max}$. To measure the defect deactivation rates (R_{deact}, during dark annealing), a slightly different double-exponential function was used:

$$NDD = a'\left(e^{-t\times R_{deact1}}\right) + b'\left(e^{-t\times R_{deact2}}\right) \quad (3)$$

where a' and b' are the pre-exponential factors. The extracted rates were used to determine the activation energies (E_a), using an Arrhenius plot fitted with a single- or double-exponential function:

$$R = a''\left(e^{-E_a/k_BT}\right) \text{ or } R = a''\left(e^{-E_{a1}/k_BT}\right) + b''\left(e^{-E_{a2}/k_BT}\right) \quad (4)$$

where R is the defect formation or deactivation rate, a'' and b'' are the pre-exponential factors, k_B is the Boltzmann constant, and T is the temperature.

3. Results and discussion

3.1. Defect formation

In Fig. 1, changes in the lifetime (at $\Delta n = 0.1 \times N_A$ where N_A is the doping concentration) and NDD of representative Ga- and In-doped samples during light soaking (0.4 suns at 80 °C) are presented. To remove the possible impact of iron (Fe) on the measurements (by forming Fe–Ga or Fe–In pairs), in addition to gettering, the samples were light-soaked at room temperature using the flash of the lifetime tester to dissociate the pairs. This was done until no change in the lifetime was observed with additional flashing (the impact of Fe on lifetime was determined to be <4% of the τ_{DA}). The initial lifetime of both the Ga- and In-doped samples is ~220 μs. The lifetime drops to 75 μs (Ga, after ~ 20,000 s) and 50 μs (In, after ~ 450,000 s). The lifetime returns to its initial value after a dark annealing step (at 180 °C). The duration of the dark annealing step needed to recover the lifetime is different for each sample and will be discussed in more detail in the next section. This suggests that the Ga- and In-doped Cz wafers are likely to have "degraded" and "annealed" states similar to the states observed in LID [13] and LeTID [22]. It has been shown that the rate and extent of LID

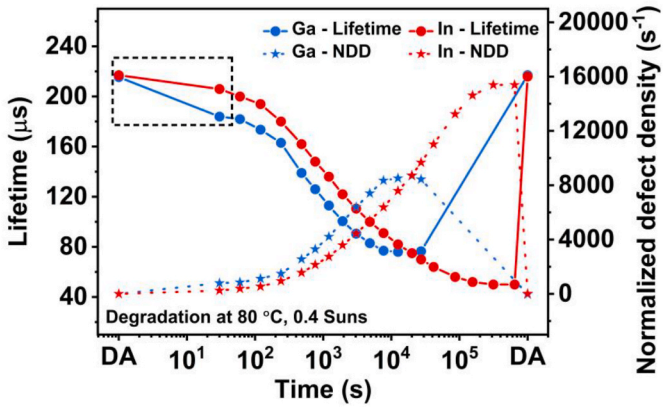

Fig. 1. Change in the lifetime (at $\Delta n = 0.1 \times N_A$) and NDD of representative Ga-, and In-doped samples during light soaking using 0.4-sun illumination intensity at 80 °C. The lifetime of the Ga-doped sample, unlike the In-doped sample, has a sharp drop in the first 30 s (marked with a black box). The solid and dashed lines are a guide to the eyes.

[1,13], as well as the extent of LeTID [23] in B-doped wafers, can be doping-dependent. It is possible that such a correlation be present for the Ga- and In-doped samples as well. Thus, care should be taken when comparing the degradation rate and extent of the Ga-doped samples and the In-doped samples. While the doping density of Ga-doped samples is 8.1×10^{15} cm^{-3} and it is almost fully ionised at 80 °C (>99%), the In-doped samples have a lower doping density (5.5×10^{15} cm^{-3}) with lower ionisation extent (~90%) at this temperature [6].

Focusing on the short time scales in Fig. 1 (marked with a black box), an abrupt decrease in the lifetime can be observed for the Ga-doped sample while such a change is not detected for the In-doped sample. To further investigate this region, two samples were degraded using a lower illumination intensity of 0.1 suns at 28 °C (Ga) and 50 °C (In). Due to the lower illumination intensity and temperature compared with the degradation condition in Fig. 1, the changes in the lifetime are slower, allowing easier monitoring of the lifetime change over shorter time scales. The choice of higher temperature for the In-doped sample was because no degradation was observed in this sample at 28 °C after 50 h of light soaking. In Fig. 2(a) and Fig. 2(b), changes in the lifetime (left *y*-axis, blue) and NDD (right *y*-axis, red) of the Ga- and In-doped samples during degradation are presented. The Ga-doped sample demonstrates a clear two-step degradation, resulting in a drop in the lifetime from 205 μs to 177 μs within a few minutes. This is then followed by a second, much slower degradation step. A two-step degradation process in Ga-doped wafers during light soaking was also reported in Ref. [16]. Furthermore, a similar two-step process has been previously reported for LeTID of B-doped multicrystalline silicon (mc-Si) wafers [24]. On the contrary, the In-doped sample seems to be quite stable until 1,000 s of light soaking and then degrades in a single stage.

To extract the activation energies of the defect formation, the light soaking process was repeated at seven temperatures between 50 °C and 155 °C and the defect formation rate was determined at each temperature. For this purpose, the NDD data (at each temperature) as a function of light soaking duration were fitted with a double-exponential function for the Ga-doped sample (R-squared > 0.99 at all temperatures), and a single-exponential function for the In-doped sample (R-squared > 0.97 at all temperatures). For the Ga-doped sample, only the activation energy of the slow step degradation was extracted, since the time constant of the fast degradation rate is smaller or in the order of the minimum measurement step of 10 s. It should be noted that in the measured temperature range, the change in the surface passivation quality is negligible with a maximum of 5% change in the J_0 at $\Delta n = 10^{16}$ cm^{-3}.

The generated Arrhenius plot is shown in Fig. 3 while the extracted activation energies are summarised in Table 1. The activation energy of LID-related defect formation in Ga-doped Cz wafers was investigated previously by Winter et al. [15]. They determined an activation energy of 0.58 ± 0.04 eV for the generation of LID-related defects (in the temperature range of 90 °C–140 °C) [15]. They also reported a deviation from this energy at temperatures below 90 °C [15]; such a deviation has not been observed in our study (in the temperature range of 50 °C–155 °C). Moreover, in Ref. [15] the degradation curves were fitted

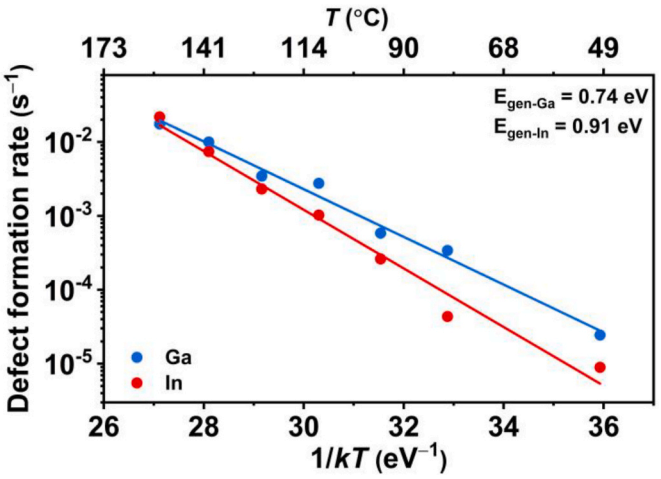

Fig. 3. Temperature dependence of the defect formation rates in Ga- and In-doped Cz wafers due to light soaking under 0.4 suns illumination intensity at 50 °C–155 °C temperature range. The investigated defect for Ga-doped wafers is the slow-formed defect. The solid lines are exponential fits to the data.

Table 1
Activation energies of the LID-related defect formation in Ga- and In-doped Cz wafers (this study), LID-related defects in Ga-doped Cz wafers [15,16].

Defect	Activation energy (eV)		
LID in Ga-doped Cz	0.74 ± 0.10 (this study)	0.58 ± 0.04 [15]	0.90 ± 0.05 [16]
LID in In-doped Cz	0.91 ± 0.15 (this study)		
LID in B-doped Cz		0.23 ± 0.02 (slow) [1]	0.475 ± 0.035 (fast) [1]

using a single-exponential function, assuming a one-step degradation process, which might have caused an error in the extracted activation energy. In another study, the activation energy of the slow step defects was determined to be 0.90 ± 0.05 eV (in the temperature range of 100 °C–160 °C) [16]. The difference between the light intensity used to induce the degradation process (0.4 suns as used by us vs. 0.7 suns in Ref. [16]) might be the source of the observed discrepancy between the extracted activation energies; it has been suggested that the degradation rate (and extent) can be affected by the intensity of the illumination used for degradation [17]. It should be noted that different degradation rates at two illumination intensities do not confirm different defect formation activation energies and further investigation is required to verify this. Another possible reason for this deviation is the difference between the resistivities of the studied samples: 0.8 Ω cm for the sample in Ref. [16] compared with 1.80 ± 0.04 Ω cm for the sample investigated here.

The value for the In-doped Cz sample is similar to the previously

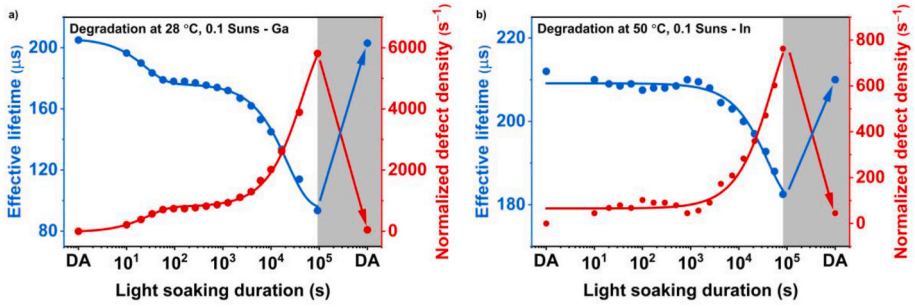

Fig. 2. Change in the lifetime (at $\Delta n = 0.1 \times N_A$) and NDD of (a) Ga-; and (b) In-doped wafers during light soaking using 0.1-sun illumination intensity at 28 °C (Ga) and 50 °C (In). The solid lines are double- (Ga) and single-exponential (In) fits to the data.

reported value for LeTID-related defect formation activation energy in B-doped mc-Si wafers (0.94 ± 0.06 eV) [24]. Compared with the Ga-doped Cz, the extracted activation energy for In-doped wafers has a slightly larger margin of error. This can be due to the temperature-dependent change in the dopant ionisation fraction, from 0.85 at 50 °C to 0.96 at 155 °C [6]. Therefore, the degradation happens with different background doping at different temperatures, which may cause a slight shift in the degradation rate. Although there is no report regarding the activation energy in In-doped wafers, interestingly, the extracted value is similar to the value reported for the Ga-doped Cz wafers in Ref. [16], despite the different doping element. It is noted that the extracted activation energies for both Ga and In wafers are different from the activation energies extracted for the BO-related LID [1], hence, it seems that a different defect causes the degradation.

3.2. Defect deactivation

It has been suggested that the generated LID- and LeTID-related defects in B-doped wafers can be deactivated with a dark annealing process [13,14]. This was also shown for Ga- and In-doped wafers in Fig. 1, where the lifetime of the samples recovered after post-LID dark annealing. To investigate the kinetics of the defect deactivation with dark annealing, a set of two fully degraded samples with Ga and In doping were dark annealed at 170 °C. The change in the lifetime (at $\Delta n = 0.1 \times N_A$) of these two samples is shown in Fig. 4. The lifetime recovery (defect deactivation) of the Ga-doped wafers during dark annealing happens in two steps, a fast process and a slow one. The former step is completed at around 1,000 s while the second step is extended up to more than 100,000 s. Similarly, the In-doped sample shows a two-step lifetime recovery throughout the dark annealing process. Neither Ga- nor In-doped samples demonstrate a reduction in the lifetime within the prolonged dark annealing time span investigated here (>100,000 s).

To extract the activation energy for the deactivation of the LID-related defects in Ga- and In-doped Cz wafers, change in the lifetime during dark annealing was measured at seven different temperatures in the range of 140 °C–200 °C (10 °C temperature intervals). Similar to the degradation, the changes in the surface passivation quality during dark annealing at these temperatures are small (<7% change in the J_0). For Ga-doped wafers, the recovery at the highest temperature (200 °C) happens after ~10 min and as it will be shown below, the lifetime of these samples is still stable at a higher temperature (230 °C) after a longer duration (16 min) of dark annealing. From the extracted lifetime, the NDD as a function of dark annealing duration curves were generated and subsequently fitted with a double-exponential function (R-squared > 0.99 at all temperatures for both doping) to extract the defect deactivation rates. The Arrhenius plots for the defect deactivation rates are provided in Fig. 5. For the extraction of the defect deactivation rate in the fast step in the Ga-doped sample, only the data up to 180 °C has been used, since at higher temperatures, the initial lifetime recovery happens in time scales close to the minimum measurement time intervals of 10 s.

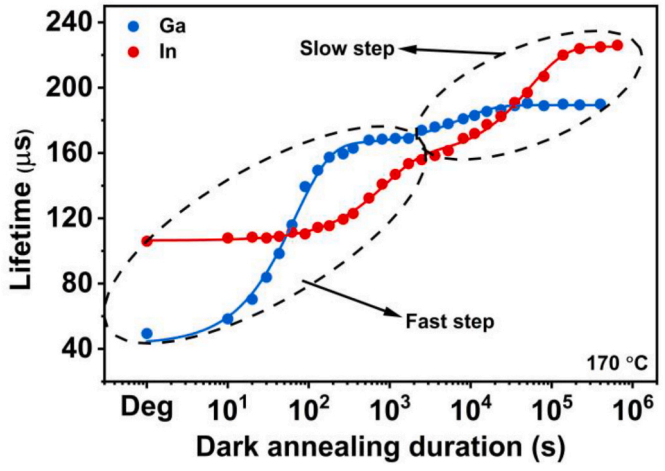

Fig. 4. Change in the lifetime (at $\Delta n = 0.1 \times N_A$) of Ga- and In-doped samples during dark annealing at 170 °C. The solid lines are double-exponential fits to the data.

The Arrhenius plot for the fast step deactivation is shown in Fig. 5(a). The extracted activation energies for the fast step of defect deactivation in the Ga- and In-doped samples are 1.61 ± 0.04 eV and 1.40 ± 0.09 eV, respectively. While only a single regime is realised for the activation energy of the fast step throughout the entire temperature range, the deactivation of defects in the slow step shows two activation energies for both dopings, as shown in Fig. 5(b). For the Ga-doped sample, the deactivation rate seems to be temperature independent for temperatures below 150 °C (use the upper *x*-axis), whereas at higher temperatures it follows an exponential increase with an activation energy of 1.86 ± 0.10 eV. For the In-doped sample, two activation energies can be extracted for two temperature ranges, 2.51 ± 0.11 eV for temperatures above ~180 °C and 0.90 ± 0.08 eV for temperatures below ~160 °C. These values are summarised in Table 2.

Considering that Ga-doped samples have two-step degradation and regeneration processes, it is not yet clear whether two sets of defects are formed and deactivated during light soaking and dark annealing, or one set of defects has a two-step formation and deactivation processes. For In-doped samples, on the other hand, it is more likely that one set of defects is formed (one-step degradation) that are then deactivated in two steps.

3.3. A three-state mechanism for LID in Ga-doped Cz silicon

In this section, we focus on Ga-doped Cz wafers which are currently the dominant material for the production of *p*-type silicon solar cells [7]. To study LID in Ga-doped wafers, it is crucial to investigate its mechanism. Previous studies on boron-oxygen (BO)-related degradation in B-doped Cz wafers have suggested a three-state model to describe the degradation behaviour in this material [13]. In this model, the two-stage degradation process (slow and fast) is considered as one step. For LeTID in mc-Si, both three- and four-state models have been suggested to describe the kinetics of the degradation [14,25]. In all of these models, the three main states are annealed, degraded, and stabilised states [13,25], while for LeTID in *p*-type mc-Si wafers, a fourth state (reservoir state) has also been suggested [14]. The four-state kinetic model suggests that a portion of the defects reaching the stabilised state (after prolonged illumination) are fully stabilised and will not return to the annealed state with dark annealing [14]. As a result, the degradation extent during consecutive illumination-dark annealing cycles decreases as more defects remain in the stabilised state after each cycle. On the other hand, dark annealing has the opposite impact. With dark annealing, the defect precursors are transferred from the reservoir state to the annealed state, meaning the increased number of precursors in the annealed state leads to a higher degradation extent [14]. Thus, the total degradation extent at each cycle depends on the combined effect of these two phenomena. Ultimately, as the reservoir is gradually depleted during consecutive 'laser annealing'-'dark annealing' cycles, the former effect becomes dominant, the number of defect precursors is decreased, and in turn, the degradation extent reduces [14]. Previously, it has been suggested by Kwapil et al. that this four-state model can also explain the observations of the LID in Ga-doped Cz wafers [17]. While, the presence of the precursor (annealed), degraded, and regenerated (stabilised) states were observed for their samples, the presence of a reservoir state was not confirmed by their measurements [17]. To investigate the mechanism governing LID in Ga-doped wafers, two sets of samples, from the Ga-1 and Ga-2, were processed through laser annealing and dark annealing cycles multiple times and the evolution of degradation extent during these cycles was monitored.

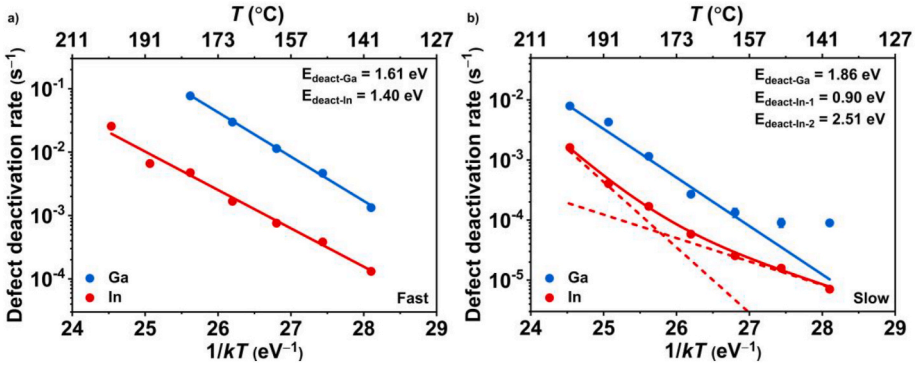

Fig. 5. Temperature-dependent defect deactivation rates of the (a) fast; and (b) slow steps in Ga- and In-doped wafers. The error bars of the extracted rates are only visible for the data points where the bar is larger than the marker size. The solid lines are single- (Ga-fast, In-fast, Ga-slow) and double-exponential (In-slow) fits to the data.

Table 2
Activation energies of the fast and slow steps of LID-related defects deactivation in Ga- and In-doped Cz wafers.

Defect	Activation energy (eV)	Temperature range
LID in Ga-doped Cz – fast step	1.61 ± 0.04	140 °C–180 °C
LID in Ga-doped Cz – slow step	1.86 ± 0.10	140 °C–200 °C
LID in In-doped Cz – fast step	1.40 ± 0.09	140 °C–200 °C
LID in In-doped Cz – slow step	2.51 ± 0.11	140 °C–200 °C
LID in In-doped Cz – slow step	0.90 ± 0.08	140 °C–200 °C

The change in the lifetime (at $\Delta n = 0.1 \times N_A$) of a representative Ga-doped Cz sample which has gone through several laser annealing-dark annealing (at 230 °C) cycles is presented in Fig. 6(a). The chosen laser annealing illumination intensity (26 suns) and temperature (140 °C), and the dark annealing temperature (230 °C) during these cycles are based on Ref [14]. The sample was dark annealed for 8 min before starting the laser annealing process of Cycles 2, 3, 5, and 6 while it had been dark annealed for 20 min before starting the laser annealing process of Cycles 4 and 7 (lifetime after dark annealing are marked with black). The dark annealing duration was selected such that the impact of the process on the transition between the stabilised and the annealed states can be easily observed. To ensure that all the defects are in the stabilised state before the first 8-min dark annealing, a full degradation and recovery of the as-fired sample were done initially (Cycle 1). The lifetime throughout a cycle drops initially reaching a maximum degradation extent (marked with red) and recovers with further laser annealing. The initial lifetime of the sample is 287 μs and it drops to ~147 μs in Cycles 2, 3, 5, and 6. The lifetime in the most degraded state (Cycles 4 and 7) is ~121 μs. The increase in the lifetime after the first cycles might be due to the hydrogenation of some bulk defects during the laser annealing process [26]. It is also observed that the lifetime after each dark annealing step drops. This is presumably due to the reduction in the surface passivation quality with dark annealing as J_0 at $\Delta n = 10^{16}$ cm^{-3} increases from ~100 fA/cm^2 at the start of the first cycle to ~120 fA/cm^2 at the end of the final cycle.

In Cycles 2 and 3, the degraded lifetime remains constant suggesting that unlike the four-state model proposed for LeTID [14], the LID-related defects do not remain in the stabilised state after dark annealing. The defects return to the annealed state with dark annealing and therefore demonstrate a similar degradation extent in Cycle 3. Moreover, if a reservoir state was present, the 8-min dark annealing before Cycle 3 would have resulted in a higher degradation extent in this cycle, as the defect precursors would transfer from the reservoir state to the annealed state. However, it is also possible that the 8-min dark annealing has not been sufficient to generate a significant density of defect precursors. Thus, after the third cycle, the sample was dark annealed for a longer duration (20 min) and went through a laser annealing-dark annealing cycle. The degradation extent increases after the prolonged dark annealing. This might be due to the release of defect precursors from a reservoir state. If that is the case, the degradation extent after another 8-min dark annealing should be higher than the degradation extent in Cycles 2 and 3. In contrast, the degradation extent is similar to the value measured in those two cycles, suggesting that no new defect precursors have been generated as a result of the prolonged dark annealing. The difference between the degradation extent after 8-min and 20-min dark annealing is possibly due to the incomplete recovery of the defects from the stabilised state to the annealed state with 8-min dark annealing. The same conclusion can be drawn from Fig. 6(b). While all the cycles following an 8-min dark annealing step show a maximum defect density of ~3300 s^{-1}, the maximum density of defects in the cycles following 20-min dark annealing is 45% higher at ~4800 s^{-1}. This also confirms that defects are not fully stabilised with prolonged illumination and defects precursors are not generated from a reservoir state during the dark annealing. The maximum change in the NDD due to the surface

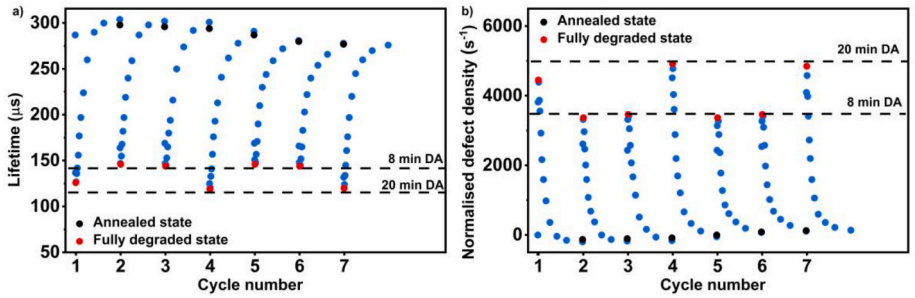

Fig. 6. (a) Lifetime (at $\Delta n = 0.1 \times N_A$) and (b) NDD of a Ga-doped Cz sample from the Ga-1 set which has gone through several dark annealing (DA, at 230 °C)-laser annealing (at 140 °C) cycles. The black dots are the initial lifetime values after the dark annealing process while the red dots are the lifetime values after full degradation. (For interpretation of the references to colour in this figure legend, the reader is referred to the Web version of this article.)

effects throughout the cycles is less than 350 s^{-1} (hence, < 11% of the total change in the NDD). Note that the dark annealing performed on this sample is done after the full recovery of the lifetime (stabilised state), while the dark annealing in the previous section was performed when the sample was in the degraded state.

To confirm this observation, a similar measurement procedure was performed on a representative sample from the Ga-2 set. Fig. 7(a) presents the lifetime while Fig. 7(b) shows the NDD of this sample. Set Ga-2 has the benefit of having a very stable lifetime throughout the process with less than 2% change in the lifetime at the dark-annealed state, throughout the dark annealing-laser annealing cycles. Thus, the prolonged dark annealing was viable. The short dark annealing cycle was reduced to 1 min (compared with 8 min for the Ga-1 sample) since it was found that both 8- and 20-min dark annealing lead to an identical degraded lifetime. This is presumably due to the faster de-stabilisation of the defects in this sample compared with Ga-1. This faster de-stabilisation might be due to the different resistivities of the two samples, however, further investigation is needed to confirm this. For Cycle 1, the sample was dark annealed for 1 min. This was followed by a laser annealing until the lifetime reached its minimum (degraded state). Then, the laser annealing was continued until the lifetime was recovered. This process [dark annealing (marked with black)-degradation (marked with red)-recovery] was repeated in six more cycles. The dark annealing step was done for 1 min before Cycles 2 and 4, and for 20 min before Cycles 3, 5, 6, and 7. As can be seen, the lifetime at the degraded state remains constant at 193 μs after the first two cycles (with 1-min dark annealing). By increasing the dark annealing duration, the degraded lifetime drops to 151 μs in the third cycle. Reducing back the dark annealing duration to 1 min returns the degraded lifetime to a similar value as in Cycles 1 and 2. In Cycles 5, 6, and 7, the dark annealing is set again to 20 min and the degraded lifetime is similar to the value measured in Cycle 3. These results confirm that despite the possible difference in the substrate and surface passivation of the Ga-1 and Ga-2 sets, (1) the stabilisation state is actually meta-stable and the defects can fully return to the annealed state with a sufficiently long dark annealing process, and (2) a reservoir state is not present for LID-related defects in Ga-doped Cz wafers, as the lifetime does not decrease with the prolonged dark annealing steps.

Based on these results, a three-state mechanism is suggested to describe the kinetics of LID in Ga-doped Cz wafers. This mechanism is shown in Fig. 8. Recombination-active defects are formed due to light soaking (**Degraded State**). However, as it was shown in Fig. 2, the degradation can happen through light soaking at relatively low temperatures (28 °C), suggesting that high temperature is not necessary for the degradation (hence, the term LeTID does not accurately describe this degradation). With dark annealing, the defects return to the **Annealed State** where they are present in their precursor form. The extracted activation energy in the previous section is the activation energy of this transformation (from the Degraded State to the Annealed State). With further light soaking, the lifetime recovers, and no degradation is

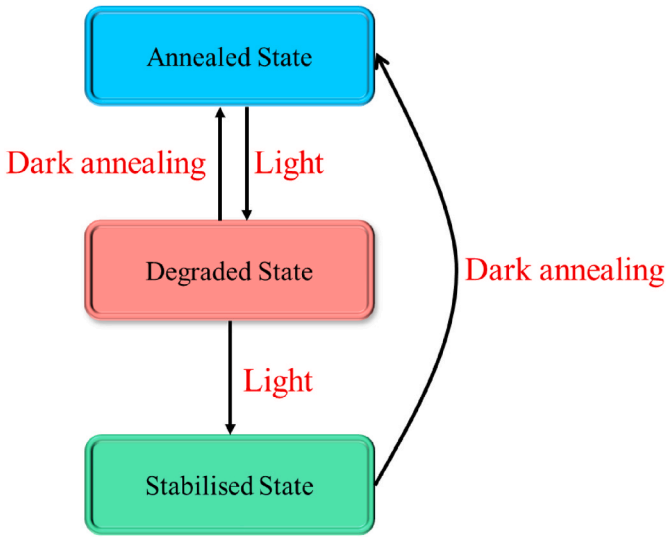

Fig. 8. Schematic of the proposed mechanism to describe LID in Ga-doped Cz wafers.

observed with prolonged light soaking (**Stabilised State**) – see Appendix 1. However, this state is not fully stable since dark annealing at high temperatures for sufficient time causes the defects to return to the Annealed State. While this mechanism is similar to the mechanism suggested for BO-related degradation, previous TIDLS investigations [27], as well as the TIDLS measurement [28] of the current sample (see Appendix 2), show that the defect causing this degradation is different from the BO-related defect. Moreover, it has also been shown that LID in Ga-doped Cz is negligible in a non-fired sample [15,16], further confirming that the LID-related defect in Ga-doped Cz is different from the BO-related defect. For both sets of samples, it was shown that the lifetime also recovers with light soaking using the halogen lamps, suggesting that these states do not depend on the illumination method (see Appendix 3).

4. Conclusions

LID in Ga- and In-doped Cz wafers was investigated through lifetime measurements. A two-stage degradation was observed in the Ga-doped Cz wafers while a one-stage degradation was noticed in the In-doped wafers. The activation energy of the defect formation was determined to be 0.74 ± 0.10 eV and 0.91 ± 0.15 eV for the LID-related defect in Ga-doped Cz (slow stage formation) and In-doped Cz, respectively. The defect deactivation through dark annealing (which transfers the defects from the degraded state to the annealed state) has been investigated as well, with both materials showing a two-stage defect deactivation. Finally, a mechanism has been suggested to explain the LID in Ga-doped

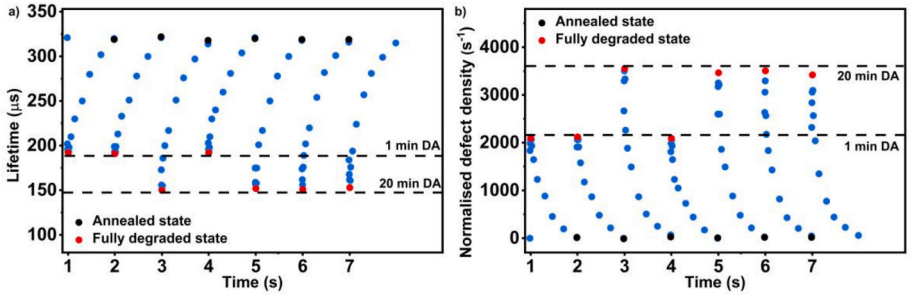

Fig. 7. (a) Lifetime (at $\Delta n = 0.1 \times N_A$) and (b) NDD of a Ga-doped Cz sample from the Ga-2 set which has gone through several DA-laser annealing cycles. The black dots are the initial lifetime values after the dark annealing process while the red dots are the lifetime values after full degradation. (For interpretation of the references to colour in this figure legend, the reader is referred to the Web version of this article.)

Cz wafers. It is proposed that three states are present: Annealed State, Degraded State, and Stabilised State. From the Annealed State, defects are generated through light soaking reaching the Degraded State. With further light soaking, the defects become inactive reaching the Stabilised State. To return the defects to the Annealed State from the Degraded or Stabilised State, dark annealing can be done. However, a longer dark annealing time duration is needed to fully return to the Annealed State from the Stabilised State compared with the Degraded State. It was concluded that the proposed mechanism for LID in Ga-doped wafers is different from the previously reported mechanism for LeTID. Future study will focus on the impact of the wafer resistivity on the degradation process.

CRediT authorship contribution statement

Saman Jafari: Writing – review & editing, Writing – original draft, Visualization, Validation, Methodology, Investigation, Formal analysis, Data curation, Conceptualization. **Mieka Figg:** Writing – review & editing, Formal analysis, Data curation. **Ziv Hameiri:** Writing – review & editing, Validation, Supervision, Resources, Project administration, Methodology, Funding acquisition, Formal analysis, Conceptualization.

Declaration of competing interest

The authors declare that they have no known competing financial interests or personal relationships that could have appeared to influence the work reported in this paper.

Data availability

Data will be made available on request.

Acknowledgment

The authors wish to thank Mr. Victor Siu (UNSW) and Dr. Shuai Nie (UNSW) for helping with the preparation of samples. This work was supported by the Australian Government through the Australian Renewable Energy Agency (ARENA) under grant 2017/RND001. The views expressed herein are not necessarily the views of the Australian Government, and the Australian Government does not accept responsibility for any information or advice contained herein.

Appendix A. Supplementary data

Supplementary data to this article can be found online at https://doi.org/10.1016/j.solmat.2022.112121.

References

[1] K. Bothe, J. Schmidt, Electronically activated boron-oxygen-related recombination centers in crystalline silicon, J. Appl. Phys. 99 (2006), 013701.
[2] P. Rosenits, T. Roth, S.W. Glunz, S. Beljakowa, Determining the defect parameters of the deep aluminum-related defect center in silicon, Appl. Phys. Lett. 91 (2007), 122109.
[3] M. Binns, J. Appel, J. Guo, H. Hieslmair, J. Chen, T. Swaminathan, E. Good, Indium-doped mono-crystalline silicon substrates exhibiting negligible lifetime degradation following light soaking, in: 42nd IEEE Photovoltaic Specialists Conference (PVSC), IEEE, 2015.
[4] S. Glunz, S. Rein, J. Knobloch, W. Wettling, T. Abe, Comparison of boron–and gallium–doped p–type Czochralski silicon for photovoltaic application, Prog. Photovoltaics Res. Appl. 7 (1999) 463–469.
[5] F.A. Trumbore, Solid solubilities of impurity elements in germanium and silicon, Bell Syst. Tech. J. 39 (1960) 205–233.
[6] L. Linares, S. Li, An improved model for analyzing hole mobility and resistivity in p-type silicon doped with boron, gallium, and indium, J. Electrochem. Soc. 128 (1981) 601.
[7] International Technology Roadmap for Photovoltaic, ITRPV, 2022.
[8] Y. Zhi, J. Zheng, M. Liao, W. Wang, Z. Liu, D. Ma, M. Feng, L. Lu, S. Yuan, Y. Wan, Ga-doped Czochralski silicon with rear p-type polysilicon passivating contact for high-efficiency p-type solar cells, Sol. Energy Mater. Sol. Cells 230 (2021), 111229.
[9] N.E. Grant, J.R. Scowcroft, A.I. Pointon, M. Al-Amin, P.P. Altermatt, J.D. Murphy, Lifetime instabilities in gallium doped monocrystalline PERC silicon solar cells, Sol. Energy Mater. Sol. Cells 206 (2020), 110299.
[10] N.E. Grant, P.P. Altermatt, T. Niewelt, R. Post, W. Kwapil, M.C. Schubert, J. D. Murphy, Gallium–doped silicon for high–efficiency commercial passivated emitter and rear solar cells, Solar RRL 5 (2021), 2000754.
[11] C. Möller, K. Lauer, A_{Si}-Si_i-defect model of light-induced degradation in silicon, Energy Proc. 55 (2014) 559–563.
[12] S. Jafari, Z. Hameiri, Investigation of light-induced degradation in Ga-and in-doped Cz silicon, in: 2021 IEEE 48th Photovoltaic Specialists Conference (PVSC), IEEE, 2021, 0814-0817.
[13] T. Niewelt, J. Schön, W. Warta, S.W. Glunz, M.C. Schubert, Degradation of crystalline silicon due to boron–oxygen defects, IEEE J. Photovoltaics 7 (2016) 383–398.
[14] T.H. Fung, M. Kim, D. Chen, C.E. Chan, B.J. Hallam, R. Chen, D.N. Payne, A. Ciesla, S.R. Wenham, M.D. Abbott, A four-state kinetic model for the carrier-induced degradation in multicrystalline silicon: introducing the reservoir state, Sol. Energy Mater. Sol. Cells 184 (2018) 48–56.
[15] M. Winter, D.C. Walter, J. Schmidt, Carrier lifetime degradation and regeneration in gallium-and boron-doped monocrystalline silicon materials, IEEE J. Photovoltaics 11 (2021) 866–872.
[16] D. Lin, Z. Hu, L. Song, D. Yang, X. Yu, Investigation on the light and elevated temperature induced degradation of gallium-doped Cz-Si, Sol. Energy 225 (2021) 407–411.
[17] W. Kwapil, J. Dalke, R. Post, T. Niewelt, Influence of dopant elements on degradation phenomena in B–and Ga–doped Czochralski–grown silicon, Solar RRL 5 (2021), 2100147.
[18] J.D. Murphy, A.I. Pointon, N.E. Grant, V.A. Shah, M. Myronov, V.V. Voronkov, R. J. Falster, Minority carrier lifetime in indium doped silicon for photovoltaics, Prog. Photovoltaics Res. Appl. 27 (2019) 844–855.
[19] C. Möller, K. Lauer, Light–induced degradation in indium–doped silicon, Phys. Status Solidi Rapid Res. Lett. 7 (2013) 461–464.
[20] E. Cho, Y.-W. Ok, A.D. Upadhyaya, M.J. Binns, J. Appel, J. Guo, A. Rohatgi, P-type indium-doped passivated emitter rear solar cells (PERC) on Czochralski silicon without light-induced degradation, IEEE J. Photovoltaics 6 (2016) 795–800.
[21] Z. Hameiri, N. Borojevic, L. Mai, N. Nandakumar, K. Kim, S. Winderbaum, Low-absorbing and thermally stable industrial silicon nitride films with very low surface recombination, IEEE J. Photovoltaics 7 (2017) 996–1003.
[22] D. Sperber, A. Herguth, G. Hahn, A 3–state defect model for light–induced degradation in boron–doped float–zone silicon, Phys. Status Solidi Rapid Res. Lett. 11 (2017), 1600408.
[23] T. Mchedlidze, J. Weber, Location and properties of carrier traps in mc–Si solar cells subjected to degradation at elevated temperatures, Phys. Status Solidi A 216 (2019), 1900142.
[24] D. Bredemeier, D. Walter, J. Schmidt, Light-induced lifetime degradation in high-performance multicrystalline silicon: detailed kinetics of the defect activation, Sol. Energy Mater. Sol. Cells 173 (2017) 2–5.
[25] K. Krauß, A.A. Brand, F. Fertig, S. Rein, J. Nekarda, Fast regeneration processes to avoid light-induced degradation in multicrystalline silicon solar cells, IEEE J. Photovoltaics 6 (2016) 1427–1431.
[26] B.J. Hallam, P.G. Hamer, S. Wang, L. Song, N. Nampalli, M.D. Abbott, C.E. Chan, D. Lu, A.M. Wenham, L. Mai, Advanced hydrogenation of dislocation clusters and boron-oxygen defects in silicon solar cells, Energy Proc. 77 (2015) 799–809.
[27] S. Jafari, M. Abbott, D. Zhang, J. Wu, F. Jiang, Z. Hameiri, Bulk defect characterization in metalized solar cells using temperature-dependent Suns-Voc measurements, Sol. Energy Mater. Sol. Cells 236 (2022), 111530.
[28] Y. Zhu, Z. Hameiri, Review of injection dependent charge carrier lifetime spectroscopy, Prog. Energy 3 (2021), 012001.